

Observation of coherent Smith-Purcell and transition radiation driven by single bunch and micro-bunched electron beams

Yifan Liang, Yingchao Du, Xiaolu Su, Dan Wang, Lixin Yan, Qili Tian, Zheng Zhou, Dong Wang, Wenhui Huang, Wei Gai, Chuanxiang Tang, I. V. Konoplev, H. Zhang, and G. Doucas

Citation: [Appl. Phys. Lett.](#) **112**, 053501 (2018);

View online: <https://doi.org/10.1063/1.5009396>

View Table of Contents: <http://aip.scitation.org/toc/apl/112/5>

Published by the [American Institute of Physics](#)

Articles you may be interested in

[SAW assisted domain wall motion in Co/Pt multilayers](#)

Applied Physics Letters **112**, 052402 (2018); 10.1063/1.5000080

[All-optical measurement of interlayer exchange coupling in Fe/Pt/FePt thin films](#)

Applied Physics Letters **112**, 052401 (2018); 10.1063/1.5004686

[High efficiency and broadband acoustic diodes](#)

Applied Physics Letters **112**, 051902 (2018); 10.1063/1.5020698

[Magnetic tunnel junctions with an equiatomic quaternary CoFeMnSi Heusler alloy electrode](#)

Applied Physics Letters **112**, 052403 (2018); 10.1063/1.5002763

[Single mode to dual mode switch through a THz reconfigurable metamaterial](#)

Applied Physics Letters **111**, 241106 (2017); 10.1063/1.5008984

[A sub-sampled approach to extremely low-dose STEM](#)

Applied Physics Letters **112**, 043104 (2018); 10.1063/1.5016192

Scilight

Sharp, quick summaries **illuminating**
the latest physics research

Sign up for **FREE!**



Observation of coherent Smith-Purcell and transition radiation driven by single bunch and micro-bunched electron beams

Yifan Liang,¹ Yingchao Du,¹ Xiaolu Su,¹ Dan Wang,¹ Lixin Yan,^{1,a)} Qili Tian,¹ Zheng Zhou,¹ Dong Wang,¹ Wenhui Huang,¹ Wei Gai,¹ Chuanxiang Tang,¹ I. V. Konoplev,^{2,a)} H. Zhang,² and G. Doucas²

¹Department of Engineering Physics, Tsinghua University, Beijing 100084, China

²JAI, Department of Physics, University of Oxford, Oxford, OX1 3RH, United Kingdom

(Received 16 October 2017; accepted 12 January 2018; published online 29 January 2018)

Generation of coherent Smith-Purcell (cSPr) and transition/diffraction radiation using a single bunch or a pre-modulated relativistic electron beam is one of the growing research areas aiming at the development of radiation sources and beam diagnostics for accelerators. We report the results of comparative experimental studies of terahertz radiation generation by an electron bunch and micro-bunched electron beams and the spectral properties of the coherent transition and SP radiation. The properties of cSPr spectra are investigated and discussed, and excitations of the fundamental and second harmonics of cSPr and their dependence on the beam-grating separation are shown. The experimental and theoretical results are compared, and good agreement is demonstrated. © 2018 Author(s). All article content, except where otherwise noted, is licensed under a Creative Commons Attribution (CC BY) license (<http://creativecommons.org/licenses/by/4.0/>). <https://doi.org/10.1063/1.5009396>

There is a growing interest in the generation of high power (kW level), narrow-band terahertz (THz) radiation (frequency ranging from 0.3 THz to 10 THz). The studies of different mechanisms of THz lasing is an active research area which addresses challenges in physics and drives the developments of other branches of science including biology, chemistry, medical science, and humanitarian studies (archaeology, study of historical artefacts including paintings and stone objects).^{1–7} One of the ways to generate high power THz radiation is to use a high energy (above 1 MeV) electron beam consisting of either a single, high-charge sub-picosecond long bunch or a number of equally spaced low-charge femtosecond micro-bunches^{8–11} (pre-bunched electron beam). There are several methods of generating coherent THz radiation using such beams including transition, diffraction, and Cherenkov mechanisms.^{9–13} However, all of them either cause a beam loss, material activation/destruction, and/or have overall a low energy conversion efficiency, i.e., from electron kinetic energy to THz radiation. A possible alternative is a THz coherent Smith-Purcell radiation (cSPr) which can be observed if an electron beam propagates above a metal grating (Fig. 1) having either a mm and a sub-mm period,^{11,14–16} preventing destruction or activation of the grating. In Fig. 1, the contour plot of the electro-magnetic field generated by a sub-picosecond electron bunch (45 MeV, 0.1 nC) propagating above (1 mm separation) the grating (0.6 mm period, 30° blazed angle) is shown. The plot is generated using the 3D PIC code Magic¹⁷ and shows excitation of surface fields on the grating and its scattering on the discontinuities (grating's edges). The inset shows the wave-form of the total electromagnetic (EM) signal measured at the point located 1 cm above the middle of

the grating. The wave-form shows the presence of coherent diffraction (first two single envelope pulses) radiation (cDR) and cSPr (oscillating, frequency chirped pulse). The grating operates as a radiator and as a dispersive media scattering radiation as defined by the dispersion relation (1) allowing stable, single frequency to be observed at a specific angle

$$\lambda = \frac{d_z}{m} (\beta^{-1} - \cos \theta). \quad (1)$$

The dispersion relation (1) links the radiation wavelength λ , the electron beam normalised velocity β , the observation angle θ , and the grating period d_z , and m is the harmonic number. It allows selecting a specific frequency ω_i with bandwidth $\Delta\omega = \omega_i/mN_{gr}$ ($N_{gr} = L_{gr}/d_z$ and L_{gr} is the grating length) by locating the output port at the correct angle θ_i with respect to the direction of propagation of the beam.^{11,14–16} It is worth noting that the beam-radiation energy conversion efficiency in the case of cSPr can be optimised for a specific application since the energy of the cSPr pulse scales according to the square of the number of periods in the grating.^{11,14–16,18–20} The spectrum of the radiation

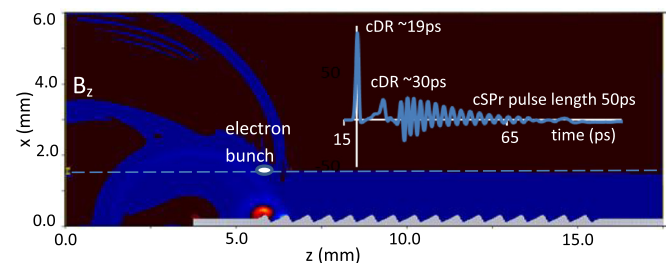


FIG. 1. A contour plot of the electro-magnetic field generated by an electron bunch propagating above a grating (0.6 mm period). The inset shows the waveform of the signal generated by the bunch propagating above the grating with cSPr (grating radiation) and cDR (edge radiation) pulses indicated.

^{a)}Authors to whom correspondence should be addressed: yanlx@mail.tsinghua.edu.cn and Ivan.Konoplev@physics.ox.ac.uk

generated by a single short (in comparison to the operating wavelength) bunch covers a broad range of frequencies, and the intensity of THz radiation in this case is limited by the bunch charge^{14–16} (i.e., the number of the electrons in the bunch) which is, in turn, limited by Coulomb repulsion. Thus, the space charge Coulomb repulsion effectively limits the output power of THz radiation, and to overcome this limitation, the modulated beam, i.e., train of low charge micro-bunches, is required. Indeed, the advantage of using the train of the multi-bunches is the possibility of operating at very high, total average charge while avoiding space charge limitations usual for the case of a single bunch. Let us consider a train of N_b electron micro-bunches with N_e electrons contained in each micro-bunch. In this case, the intensity of radiation generated in a solid angle by such a train can be presented as

$$\left(\frac{dI}{d\Omega}\right)_{train} = \left(\frac{dI}{d\Omega}\right)_1 (N_e N_b S_{inc}(\omega) + N_e N_b (N_b N_e - 1) S_{coh}^2(\omega)), \quad (2)$$

where S_{inc} and S_{coh} are the incoherent and coherent form factors (normalized to unity), respectively. When the length of an individual micro-bunch is shorter as compared with the radiation wavelength, the first term in brackets $N_e N_b S_{inc}$ becomes negligible in comparison to the second term in Eq. (2) which is proportional to $(N_e N_b)^2$, and coherent Smith-Purcell radiation (cSPr) is observed. The expression (2) is written for a train of micro-bunches and $S_{coh}(\omega) \sim \left[\frac{\sin(\omega N_b T/2)}{\sin(\omega T/2)}\right]$, indicating that the bandwidth of the spectral line generated by the train of micro-bunches is $\Delta\omega_0 = \omega_0/N_b$, where $\omega_0 = 2\pi/T$ and T is the interval between the micro-bunches (see also Refs. 10–12). One notes that the general form of Eq. (2) is the same for cSPr and cTr with only a difference in the first term $(dI/d\Omega)_1$ which is specific for each type of radiation. One of the aims of the experiments was to compare widths of the spectral lines of cTr and cSPr signals observed by a single detector at a specific position in a far field zone, showing that the cTr spectral line width is proportional to N_b^{-1} , while the cSPr spectral line width is proportional to N_{gr}^{-1} (unless $N_b > N_{gr}$). In both cases, the detectors were positioned at 90° to the beam trajectory (Fig. 2). We note that the cTr was generated from the aluminium target (Fig. 2), which was removed during the cSPr studies. If a pre-bunched electron beam is used [Ref. 11a], the spectral characteristics of the output radiation will strongly depend on the periodicity of the micro-bunches which is challenging to control. Nevertheless, the stability of the frequency generation can be very important for a number of applications,^{1–7} and the use of the SP mechanism of the radiation generation allows the frequency stability issue to be solved in a rather simple and elegant manner. Indeed, it is understood that the dispersion relation [Eq. (1)] is valid for a pre-bunched beam and locating the output port at a specific angle will “lock” the output frequency of the observed signal. In this letter, we report experimental observations of both cSPr and coherent transition radiation (cTr) generated by electron beams consisting either of a single femtosecond (fs) bunch or a periodic train of fs-long micro-bunches (λ_b is the distance between the micro-bunches). The

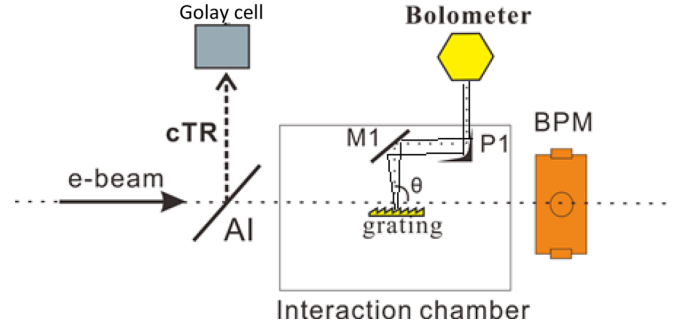


FIG. 2. The schematic of the experimental setup. The Al film before the chamber is used to produce cTr and can be moved in and out. An electron beam of approximately $100\mu\text{m}$ diameter passing over a copper grating generates cSPr which is collected by a system of flat and parabolic mirrors at 90° and subsequently measured using a bolometer.

features of the observed cSPr and cTr will be compared, and the results observed will be discussed.

The experiments were carried out at the Tsinghua Thomson scattering X-ray source (TTX)^{21,22} (Tsinghua University, Beijing, China). The facility allows the generation of high-current modulated electron beams, i.e., a train of micro-bunches with tunable periodicity²² (see Ref. 22 for the beam parameters as well). After the injection into the accelerator, the beam undergoes additional acceleration and passes through dispersive and compression stages where nonlinear longitudinal space charge effects lead to the formation of the micro-bunched electron beam. TTX facility is also capable of generating single fs-electron bunches, whose longitudinal profile can be controlled by a chicane located before the THz chamber, making TTX extremely suitable for THz studies. The beam’s total charge can be varied from a few pC to 1 nC, and the maximum beam energy is around 45 MeV. The experimental setups are shown in Fig. 2 showing two detectors (Golay cell and Bolometer) which were placed outside the vacuum chamber and positioned at observation angle $\theta = 90^\circ$ toward the beam trajectory. The measurements were performed using cTr and cSPr stages, and in both cases, a single fs electron bunch and a train of seven fs-long micro-bunches with a variable period were used. To study cSPr, two 10 mm wide and 110 mm long gratings of periods 0.3 mm and 0.6 mm and with blaze angles $\alpha = 45^\circ$ and 30° , respectively, were used. To start, the single bunch mode was used to generate cSPr from the 0.3 mm period grating aiming at the observation of the cSPr intensity dependence on the bunch compression at the grating position. The magnetic field of the chicane controls the electron bunch compression (the bunch length), and it was adjusted by varying the chicane current to observe the highest intensity, and the optimal (for cSPr signal generation) bunch parameters were achieved for the chicane current around $I_{ch} = 35\text{ A}$ [Fig. 3(a)]. A further increase in the chicane current led to a decrease in the amplitude of the radiated signal. In Fig. 3(a), the dependence of the intensity of the cSPr signal (from the 0.3 mm period grating) at around 1 THz on the chicane current is demonstrated. For a chicane current in the range 20 A–32 A, there is an approximately exponential increase in the intensity, which reaches a “plateau” in the region 32 A–37 A. Thereafter, there is an approximately exponential decrease in the signal amplitude. One notes that the

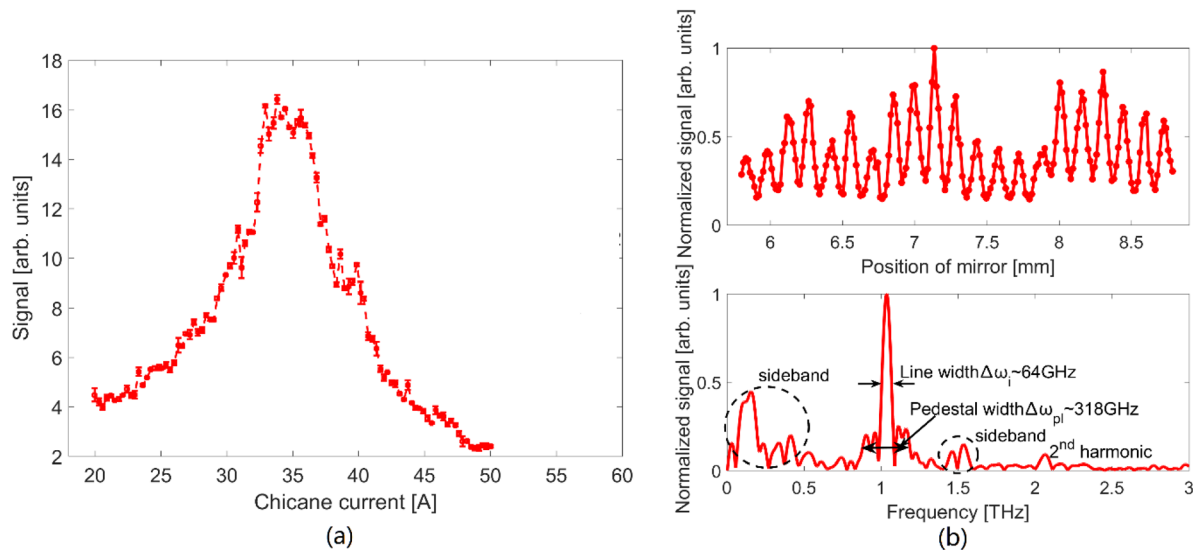


FIG. 3. (a) Amplitude of the normalised cSPR signal measured at approximately 1 THz versus the chicane current for the 0.3 mm period grating. (b) A typical interferogram and spectrum of the cSPR signal measured when the chicane current was set at 35 A.

dependence of the cSPR signal on the chicane current reflects the dependence of this signal's amplitude on the length of the bunch for a given frequency previously predicted and expected^{14–16,18–20} but not yet measured. To measure the frequency of the cSPR signal, the Michelson interferometer was used and the interferogram (top plot) and frequency of the signal are shown in Fig. 3(b). The spectrum broadening, $\Delta\omega_l \cong 64$ GHz [Fig. 3(b)] instead of the expected 3 GHz, is explained by the width of the acceptance apertures of the THz detectors and the THz chamber output optics $\Delta\theta_i = \pm 1.75^\circ$. The appearance of the side-bands [Fig. 3(b), dotted circles] in the spectrum can be explained by the cDR (see Fig. 1), manifesting itself by the appearance of high and low frequency sidebands outside the expected cSPR line and by the increased width of the pedestal. To investigate further the peculiarities of cSPR, the dependence of the second

harmonic [Fig. 3(b), observed from the 0.6 mm-period grating and 700 pC bunch] intensity on beam grating separation was studied. The use of 0.6 mm grating allowed us to stay in the operating frequency range of the detectors. In Fig. 4, the spectrum of the cSPR signal, measured at an observation angle $\theta = 90^\circ$, is shown. The fundamental and the second harmonics were observed, and the insets show the dependence of the sum of the intensities of both harmonics versus beam grating separation x_0 (top figure) and the dependence of the second harmonic intensity on x_0 (bottom inset). In the latter case, the fundamental harmonic was filtered out using a narrow-band-pass filter. The insets show the exponential decay of the amplitude of the signals with increasing x_0 . The expression for the best fit line in the case of second harmonic is $y = 12.5e^{-x/1.24} + 1.74$ which agrees well with the expected value of coupling parameter $\lambda_e \sim 1.2$.^{14–16}

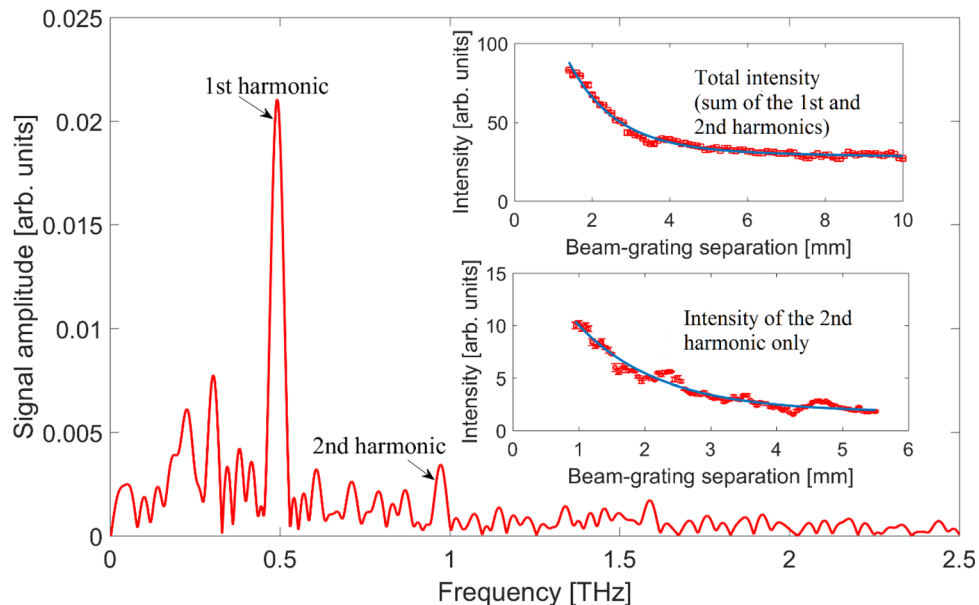


FIG. 4. cSPR spectrum from the 0.6 mm period grating. The inset illustrates the measured signal versus beam-grating separation for the total energy and the filtered second order (1 THz), respectively.

To study THz lasing by a micro-bunched beam, the accelerator was tuned to produce trains of seven tens of femtosecond long, electron micro-bunches. The spectra of the cTr and cSPr (observed from both the 0.3 mm and the 0.6 mm gratings at $\theta = 90^\circ$) are shown in Figs. 5(a) and 5(b), respectively. These were generated by the micro-bunch trains of periodicities 1 ps and 1.2 ps, respectively. In Fig. 5(a), the spectrum of the cSPr signal (solid red line) is narrower ($\Delta\omega_i \cong 64$ GHz), and it has no sidebands as compared with the cTr signal (dashed black line, $\Delta\omega_0 \cong 160$ GHz). The difference between the spectra shown in Fig. 3(b) (single bunch generated) and Fig. 5(a) illustrates that the amplitude of cDR in the second case is much lower, and it does not affect the cSPr spectrum. Also, a comparison of Figs. 3(b) and 5(a) demonstrates that the frequency observed at 90° and its line width are independent of the bunch train structure (single bunch or micro-bunches) and depend only on the grating parameters. Indeed, the amplitude of the spectral line is a function of beam parameters,^{11,20,23} but its position and width depend only on the grating parameters (unless $N_b > N_{gr}$). In a separate experiment, a micro-bunch train of periodicity 1.2 ps was driven over the 0.6 mm grating (instead of the 0.3 mm grating). The change in gratings was done in order to improve the separation of the spectral lines (better visualisation). As in the previous experiment, both cTr [Fig. 5(b), dashed lines] and cSPr [Fig. 5(b), solid red line] signals were measured. Both interferograms (top figure) and spectra (bottom figure) are shown in Fig. 5(b). We note that the width of the cSPr signal spectral line did not change ($\Delta\omega_i \cong 64$ GHz), showing output optics and interferometer limited resolutions. There are also clear differences of the line widths of the cTr spectra shown in Figs. 5(a) and 5(b) ($\Delta\omega_0 \cong \omega_0/N_b$). In both cases, the number of the macro-bunches was $N_b = 7$, but the micro-bunch spacing was different, 1.0 and 1.2 ps, respectively [$\omega_0 \cong 1$ THz, 0.83 THz, see Figs. 5(a) and 5(b), respectively]. There are clear differences between two spectra (compare side bands and pedestals). In Fig. 5(b), the spectral width of the pedestal of the cTr signal at the level above 0.1 of the

amplitude is broader as compared with the cSPr pedestal. The spectral line width of the cSPr is $\Delta\omega_i \cong 64$ GHz, while the width of the cTr line changed from 160 GHz when the micro-bunch spacing was 1.0 ps to about 80 GHz when this spacing was increased to 1.2 ps [Figs. 5(a) and 5(b)]. This line width variation could be explained by a variation of the number of well-formed micro-bunches.²² Also, in the cSPr spectrum, the presence of the second harmonic is clear, with an amplitude of about 20% that of the fundamental. We note that shifting the micro-bunch train periodicity to 1.2 ps (0.83 THz) while carrying out the cSPr signal measurements at 0.5 THz [Fig. 5(b)] resulted in a decrease in the amplitude of cSPr fundamental harmonic²³ which became comparable with the second harmonic. Overall comparing the results, we see that the cTr has a relatively broader spectrum with sidebands and a maximum located at 0.83 THz (1.2 ps micro-bunch spacing), while the cSPr spectrum line is still narrower and located at 0.5 THz, which corresponds to the operating wavelength $\lambda = d_z$ defined by the dispersion relation [Eq. (1)]. In both cases [Figs. 5(a) and 5(b)], the position and width of cTr spectra (driven by a train of micro-bunches) are defined by the periodicity of the micro-bunches and their number, while in the case of the cSPr, it solely depends on the period of the gratings. The independence of the spectrum on the beam parameters makes the cSPr attractive for applications where spectrum stability and narrow line width are required, while the dependence of the cSPr intensity on grating length makes it also attractive for high power applications.

To conclude, we report the results of experiments that compared the spectral properties (line position and its width) of cSPr and cTr THz radiation generated using a 45 MeV beam with a total charge up to 700 pC, and a transverse dimension of $\sim 100 \mu\text{m}$ was used. To generate the radiation, the beam was delivered to the THz chamber either in the single-bunch or in the micro-bunch modes, and in the latter case, the spacing of the fs-long micro-bunches could be varied between 1.0 and 1.2 ps. We demonstrated that the cSPr intensity varies with the change in the bunch compression,

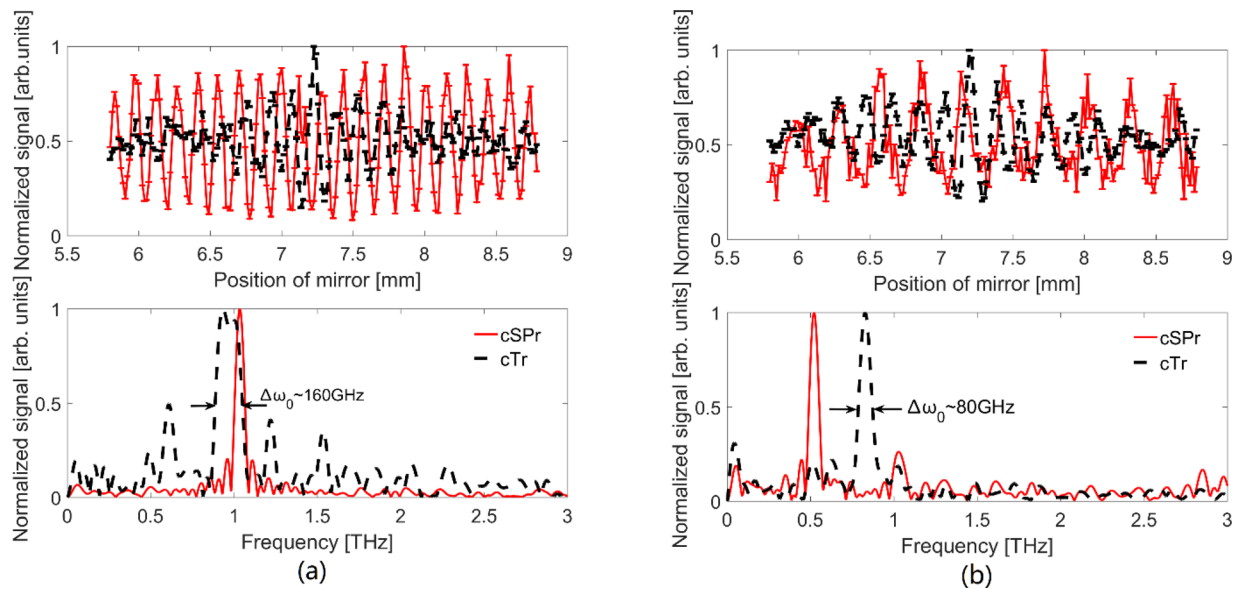


FIG. 5. Comparison of the spectra of cSPr (solid lines) and cTr (dashed lines) for (a) the grating of the 0.3 mm period and micro-bunch train of 1 ps periodicity and (b) the grating of the 0.6 mm period and micro-bunch train of 1.2 ps periodicity.

i.e., the bunch length and excitation of the second harmonic were also observed. We show that, unlike cTr, the cSPR spectrum line position and its width measured at a specific observation point do not depend on the periodicity of the micro-bunch train but are defined by the grating parameters, while (as expected from Ref. 23) the amplitude of the spectral line is a function of the periodicity of the micro-bunches. The reported results of the experiments should further advance the development of THz sources and help in bridging the “THz gap”.²⁴

This work was supported by the National Natural Science Foundation of China (NSFC Grant Nos. 11475097, 11375097, and 11435015) and the National Key Scientific Instrument and Equipment Development Project of China (Grant No. 2013YQ12034504). I.V. Konoplev would like to acknowledge the partial support of the project from the STFC UK through PRD Grant ST/M003590/1 and the Leverhulme Trust through the International Network Grant IN-2015-012. H. Zhang would like to thank NUDT (China) for supporting his DPhil project.

¹W. L. Chan, J. Deibel, and D. M. Mittleman, *Rep. Prog. Phys.* **70**, 1325–1379 (2007).

²K. Fukunaga, Y. Odawa, S. Hayashi, and I. Hosako, *IEICE Electron. Express* **4**(8), 258–263 (2007).

³K. Krügener, M. Schwerdtfeger, S. F. Busch, A. Soltani, E. Castro-Camus, M. Koch, and W. Viöl, *Sci. Rep.* **5**, 14842 (2015).

⁴S. S. Dhillon, M. S. Vitiello, E. H. Linfield, A. G. Davies, M. C. Hoffmann, J. Booske, C. Paoloni, M. Gensch, P. Weightman, G. P. Williams, E. Castro-Camus *et al.*, *J. Phys. D: Appl. Phys.* **50**, 043001 (2017).

⁵H. A. Hafez, X. Chai, A. Ibrahim, S. Mondal, D. Férachou, X. Ropagnol, and T. Ozaki, *J. Opt.* **18**, 093004 (2016).

⁶G. P. Williams, *Rep. Prog. Phys.* **69**, 301–326 (2006).

⁷F. Garet, M. Hofman, J. Meilhan, F. Simoens, and J.-L. Coutaz, *Appl. Phys. Lett.* **105**, 031106 (2014).

⁸J. H. Booske, *Phys. Plasmas* **15**, 055502 (2008).

⁹G. L. Carr, M. C. Martin, W. R. McKinney, K. Jordan, G. R. Neil, and G. P. Williams, *Nature* **420**, 153–156 (2002).

¹⁰S. Antipov, M. Babzien, C. Jing, M. Fedurin, W. Gai, A. Kanareykin, K. Kusche, V. Yakimenko, and A. Zholents, *Phys. Rev. Lett.* **111**, 134802 (2013).

¹¹A. Gover, *Phys. Rev. Spec. Top.-Accel. Beam* **8**, 030701 (2005); H. L. Andrews, F. Bakkali Taheri, J. Barros, R. Bartolini, V. Bharadwaj, C. Clarke, N. Delerue, G. Doucas, N. Fuster-Martinez, M. Vieille-Grosjean, I. V. Konoplev *et al.*, *Phys. Rev. Spec. Top. -Accel. Beam* **17**, 052802 (2014).

¹²P. Piot, Y.-E. Sun, T. J. Maxwell, J. Ruan, A. H. Lumpkin, M. M. Rihaoui, and R. Thurman-Keup, *Appl. Phys. Lett.* **98**, 261501 (2011).

¹³S. Antipov, C. Jing, M. Fedurin, W. Gai, A. Kanareykin, K. Kusche, P. Schoessow, V. Yakimenko, and A. Zholents, *Phys. Rev. Lett.* **108**, 144801 (2012).

¹⁴G. Doucas, V. Blackmore, B. Ottewell, C. Perry, P. G. Huggard, E. Castro-Camus, M. B. Johnston, J. L. Hughes, M. F. Kimmit, B. Redlich, and A. van der Meer, *Phys. Rev. ST Accel. Beams* **9**, 092801 (2006).

¹⁵D. V. Karlovets and A. P. Potylitsyn, *Phys. Rev. ST Accel. Beams* **9**, 080701 (2006).

¹⁶R. Bartolini, C. Clarke, N. Delerue, G. Doucas, and A. Reichold, *J. Instrum.* **7**, P01009 (2012).

¹⁷A. J. Woods and L. D. Ludeking, <http://www.orbitalatk.com/magic/description.aspx> for PIRS, Kuala Lumpur, Malaysia (2012); P. Zhang, L. K. Ang, and A. Gover, *Phys. Rev. Spec. Top.-Accel. Beam* **18**, 020702 (2015).

¹⁸O. Haerlé, P. Rullhusen, J.-M. Salomé, and N. Maene, *Phys. Rev. E* **49**, 3340 (1994).

¹⁹Y. Shibata, S. Hasebe, K. Ishi, S. Ono, M. Ikezawa, T. Nakazato, M. Oyamada, S. Urasawa, T. Takahashi, T. Matsuyama, K. Kobayashi, and Y. Fujita, *Phys. Rev. E* **57**, 1061 (1998).

²⁰J. Urata, M. Goldstein, M. F. Kimmitt, A. Naumov, C. Platt, and J. E. Walsh, *Phys. Rev. Lett.* **80**, 516 (1998); S. E. Korbly, A. S. Kesar, J. R. Sirigiri, and R. J. Temkin, *Phys. Rev. Lett.* **94**, 0548031 (2005); A. Gover, E. Dyunin, Y. Lurie, Y. Pinhasi, and M. V. Krongauz, *Phys. Rev. ST Accel. Beams* **8**, 030702 (2005).

²¹Y. Du, L. Yan, J. Hua, Q. Du, Z. Zhang, R. Li, H. Qian, W. Huang, H. Chen, and C. Tang, *Rev. Sci. Instrum.* **84**, 053301 (2013).

²²Z. Zhang, L. Yan, Y. Du, Z. Zhou, X. Su, L. Zheng, D. Wang, Q. Tian, W. Wang, J. Shi, H. Chen *et al.*, *Phys. Rev. Lett.* **116**, 184801 (2016).

²³H. Zhang, I. V. Konoplev, A. J. Lancaster, H. Harrison, G. Doucas, A. Aryshev, M. Shevelev, N. Terunuma, and J. Urakawa, *Appl. Phys. Lett.* **111**, 043505 (2017).

²⁴J. M. Chamberlain, *Philos. Trans. R. Soc., London A* **362**, 199–213 (2004).